ECI Symposium Series, Volume RP5: Proceedings of 7th International Conference on Heat Exchanger Fouling and Cleaning - Challenges and Opportunities, Editors Hans Müller-Steinhagen, M. Reza Malayeri, and A. Paul Watkinson, Engineering Conferences International, Tomar, Portugal, July 1 - 6, 2007

FOULING MITIGATION WITH SYNTHETIC FIBRES IN A $CASO_4$ SUPERSATURATED SOLUTION

M. Rost[1] and G. G. Duffy[2]

[1] Institute of Thermodynamics and Thermal Engineering, University of Stuttgart, Germany, matt.rost@web.de
[2] Department of Chemical and Materials Engineering, University of Auckland, New Zealand, gg.duffy@auckland.ac.nz

ABSTRACT

Wood pulp fibre suspensions and model synthetic fibre suspensions have been shown previously to mitigate effectively calcium sulphate fouling in heat exchangers. Fibre flexibility was found to be a decisive fibre property in fouling mitigation. Adding fibres to a fouling fluid is environmentally benign and can be applied during operation without shutting down the heat exchanger. Because polymer fibres are more robust in a hostile environment, further work was initiated with two types of rayon fibre and one acrylic fibre of the same fibre length.

Experiments were performed at both constant and varying fibre volume concentrations. The more flexible rayon fibres in suspension produced lower ultimate-fouling resistance values than the stiffer acrylic fibres. Fibres were embedded in the fouling layer and it is believed that this mechanism contributed to the overall fouling resistance and was a counterpart to the positive effects of fibres mitigating fouling. The more flexible fibres momentarily form visco-elastic bundles that can 'absorb' hydrodynamic shear forces, modify the turbulent stresses, and lower the fouling matter removal rate. Stiff fibres embedded in the deposit protrude into the bulk flow and entrap more fibres as they are less likely to deflect, bend, and be flattened by the shear stresses near the wall.

INTRODUCTION

Small amounts of cellulosic wood pulp fibres have been shown to mitigate fouling in supersaturated calcium sulphate solutions in heat exchangers (Middis, et al., 1998). Research over almost a decade at the University of Auckland has shown that flexible fibres actually augment heat transfer, increase the *induction period* t_D, and can limit the level of fouling after it onsets.

The flow of fibre suspensions is unique. The flexible, strongly-asymmetrical 'particles' modify the turbulence structure and produce drag reduction at high flow rates. Fibres bend, rotate, collide, and momentarily entangle at moderate shear rates. Various flow regimes are observed that are different from other particulate suspensions and other non Newtonian systems. The extent of the differences depends on fibre properties, fiber concentrations and flow conditions. Fibres in pipe flow interfere with turbulent eddies near the wall, changing the thickness of the hydrodynamic and thermal boundary layers and hence modify pressure drop as well as heat and mass transfer.

Middis et al. (1998) were the first in the group of workers at the University of Auckland to observe that wood pulp fibres are efficient in mitigating fouling, even at small concentrations of 0.05 mass percent. Subsequently to this promising result, Kazi et al. (2001) conducted many experiments with fibre suspensions of long softwood and short hardwood fibres at varying concentrations, where they found the latter fibres more efficient in mitigating fouling. At a fibre concentration of 0.25 mass percent, no fouling was observed for 46.5 days and the experiment was terminated.

MacShane (2004) used synthetic fibres instead of wood pulp fibres with the objective of finding the characteristics of the most effective fibres in mitigating fouling. Synthetic fibres have advantages as their geometrical and material properties are constant. In contrast naturally occurring, hollow, wood pulp fibres are biodegradable, have wide distributions of properties, and can collapse to form ribbon-like structures. Model fibres enable more systematic investigations of the effects of fibre properties to be investigated and are mostly inert and often reusable (e.g. water cooling loop). MacShane found the flexible fibres more efficient as they produced lower ultimate fouling resistance levels.

In this work, experiments with acrylic and rayon fibres were conducted to broaden and confirm the knowledge already found by the previous workers on this topic. Acrylic is a pure synthetic material. Rayon is cotton-like, yet is a man-made material. Both fibre materials had not been investigated with respect to fouling mitigation before. This work centres on fibre flexibility (determined both from geometrical dimensions and material properties), as it was found by both Kazi et al. and MacShane to be a decisive but ambiguous fibre property influencing fouling.

EXPERIMENTAL

Floop Loop

A diagram of the experimental apparatus used in this work and by the former workers from Kazi et al. (2001) onwards is shown in *Fig. 1*.

The main parts of the test rig were a tank (1), a tank agitator (2), two cooling-coil heat exchangers (3) in the tank, a centrifugal pump (4), a magnetic volume flow meter (5), and the heated fouling test section (6). A recycle loop made it possible to circulate the fluid directly back into the tank. Fibres could be dispersed homogenously during the experimental preparation process using the recycle system.

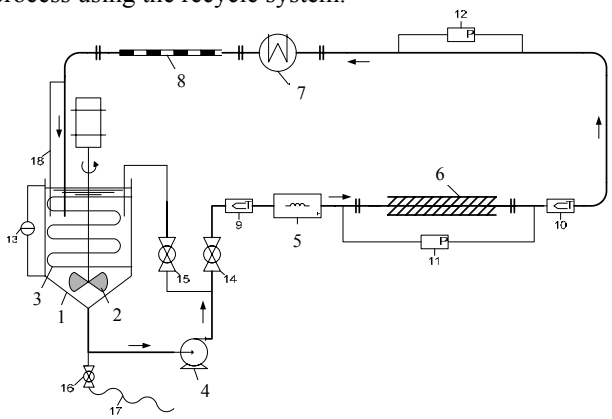

Fig. 1: Diagram of the heat transfer flow loop

The Fouling Test Section

A longitudinal cross-sectional view with all dimensions of the test section steel pipe is shown in *Fig. 2.* The test section pipe was made from 316L stainless steel with an overall length of 2000mm and an inside diameter of 49.25mm. The 900mm long heated part of the pipe was 'thermally separated' from the other pipe section by narrowing the wall with 10mm wide cut grooves at each end of the test section. Nine Watlow (MB2EJN1) band heaters were clamped around the test section with a longitudinal gap between each band heater of approximately 6mm.

The thermocouples measuring the surface temperature of the pipe were embedded in the pipe wall by cutting four 110mm-long grooves along the heated section as deep as possible without disturbing the inner surface.

The Wilson plot method was used to calculate the actual internal surface temperatures. Two K-type thermocouples were installed in the flow upstream and downstream of the test section to obtain the bulk temperatures.

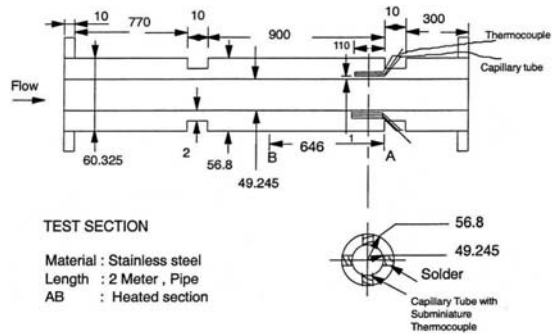

Fig. 2: Longitudinal cross-sectional view of the experimental test section (Kazi, 2001) (point 6 in *Fig. 1*).

Data Acquisition

All the measurement devices were connected to two hardware units each with eight input channels that could be read five times a second with 16 bit resolution. A customary PC collected, processed, and stored the appropriate data by the means of a data acquisition software tool called 'Picolog'. During the experiment the tool was set to retrieve and store the data every 5 minutes. The data were analysed and consolidated graphically by importing them to Microsoft Excel.

Experimental Procedure

The procedures adopted in this work are well established for this type of fouling research and are described in detail elsewhere (e.g. Bansal and Müller-Steinhagen, 1993; Kazi, 2001).

The calcium sulphate solution was prepared using calcium nitrate ($Ca(NO_3)_2 \cdot 4H_2O$) and equimolar amounts of sodium sulphate (Na_2SO_4). The chemicals added react as follows:

$$Ca(NO_3)_2 \cdot 4H_2O + Na_2SO_4 \rightarrow CaSO_4 \cdot 2H_2O + 2NaNO_3 + 2H_2O$$

This preparation method was used by previous workers as well. A $CaSO_4$-concentration of 3.6g/l was found (Kazi, 2001) to promote sufficient deposition on the heated pipe surface to perform experiments in a reasonable time without precipitation of $CaSO_4$-particles in the bulk solution.

The appropriate amount of fibres was evenly distributed in the water-filled tank with the agitator running to give the specified fibre concentration before the chemicals were added to the tank. During the experiment the Ca^{2+}-ion concentration was determined by EDTA-titration every 10 to 12 hours. The experiment was left to run until there was virtually no further change in the heat transfer coefficient (usually 4 to 7 days).

Experimental Parameters

The experimental conditions and other parameters are presented in *Table* 1.

Table 1: Standard experimental parameters

Parameter	
Bulk velocity v	0.4m/s
Reynolds number at v = 0.4m/s	28,700
Bulk temperature T_b	40°C
Wall temperature T_w	60°C
$CaSO_4$-concentration	3.6g/l
Clean heat transfer coeff. α_{clean}	1,754W/m^{2}K
Fibre volume concentration $C_{f,vol}$	0.075%-0.125%, Traces
pH of suspension/solution	7.5
Fibres used	rayon, acrylic

The values for the *current heat transfer coefficients* α were calculated from the heat flux density $\dot{q}$ and the temperature difference between the wall of the heated section T_w and the bulk fluid T_b according to *eq. 1*. The heat flux density was determined from the power supplied to the heaters and the surface area of the test section:

$$\alpha = \frac{\dot{q}}{(T_w - T_b)} \qquad (1)$$

The thermal *fouling resistance* R_f was calculated according to *eq. 2* from the reciprocal values of the current heat transfer coefficient α and the initial heat transfer coefficient α_0:

$$R_f = \frac{1}{\alpha} - \frac{1}{\alpha_0} \qquad (2)$$

Experimental and Investigational Objectives

Considerable knowledge of fouling mitigation and parameters relating to fibre properties and flow conditions has been obtained from previous research. The fibre mass concentration of wood pulp fibres was varied by Middis et al. (1998) and Kazi et al. (2001) who obtained enhanced fouling mitigation with increasing concentration. In addition, Kazi et al. conducted experiments with various fibre types of different mean-length distributions, cross-sectional dimensions (‘diameters’), and stiffness levels. They found that the shorter and stiffer fibres were more efficient in mitigating fouling than the longer and more flexible ones.

With synthetic fibres, MacShane (2004) was able to vary fibre properties in a systematic way. She found that stiffer fibres produced a longer induction period t_D and roughness delay period t_R, but generally caused higher asymptotic fouling resistances $R_{f,\infty}$ at a constant mass concentration (see notation in *Fig. 3*). As Kazi et al. (with wood pulp) and MacShane (with synthetic fibres) found both corresponding and contradictive results regarding fibre flexibility, it was proposed to examine this fibre property more closely to gain more knowledge on its affect on fouling.

Fibres used

Three fibre types were used: two types of rayon fibre and one acrylic fibre. Fibre length was the same for all fibres. One of the rayon fibres and the acrylic fibre had similar diameters. Four parameters were used to specify fibre stiffness and classify fibre types based on material properties and/or geometrical dimensions. These parameters are:

- the length-to-diameter ratio L'/D ,
- the area moment of inertia $I_{0,}$
- the calculated stiffness $S_{calc} = E \cdot I_o$, and,
- the deflection (-per-unit-force) w'
  $w' = w/F = L'^3/(48 \cdot S_{calc})$.

The appropriate values for the different fibre types are listed in *Table 2*.

Table 2: Calculated fibre properties describing flexibility and stiffness.

		Fibre flexibility		Fibre stiffness	
	Fibre name	w’ [km/N]	L’/D [-]	S_{calc} 10^{-12} [Nm^2]	I_0 10^{-21} [m^4]
L’ = const.	Rayon I*	2.22	127.9	0.287	19.41
	Rayon II*	0.83	98.5	0.820	54.65
	Acrylic	0.030	168.0	11.8	7.82

*swelled

The acrylic fibre type is the most flexible in terms of the *L'/D ratio* and the area moment of inertia I_0. Based on the deflection w’ and the calculate fibre stiffness S_{calc} the order is reversed. As the latter-mentioned parameters include the geometrical aspects of the fibre’s flexibility and stiffness as well as the modulus E (which describes the fibre’s inherent stiffness), they are reflecting the real fibre flexibility and stiffness more accurately. Hence, the acrylic fibres are considered to be the stiffest fibres, followed by Rayon II. The most flexible fibre type is Rayon I, which has w' a value of 2.22 km/N, the lowest S_{calc} value of $0.287 \cdot 10^{-12}$ Nm^2.

Typical Fouling Curves

A typical asymptotic fouling curve of $CaSO_4$-fouling, where the surface temperature of the heat transferring surface is kept constant is depicted in *Fig. 3*.

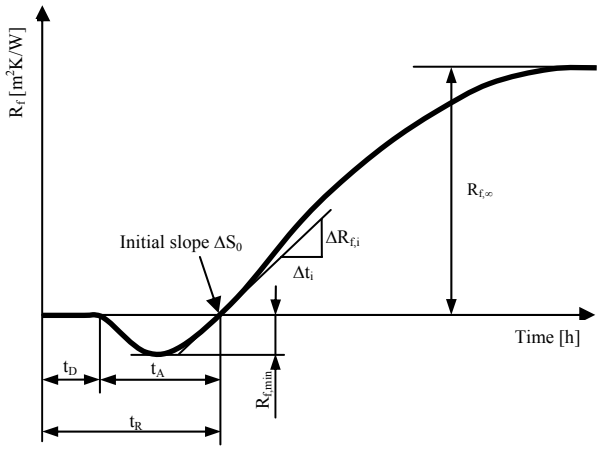

Fig. 3: Typical development of fouling resistance over time from a $CaSO_4$ super-saturated solution with a constant temperature of the heat transferring surface, hence variable heat flux and its parameter.

The fouling parameters of the curves are defined as follows:

t_D = Induction period/time
t_A = Period of heat transfer augmentation
t_R = Roughness delay period
$R_{f,min}$ = Maximum of heat transfer augmentation
ΔS_0 = Initial slope
$R_{f,\infty}$ = Ultimate fouling resistance

RESULTS

Wood Pulp Fibres

The first experiment with fibres was conducted with long-fibre bleached Kraft pine pulp fibres at a fibre mass concentration of 0.1% as a reference to previous work. The results are shown in *Fig. 4* for comparison where the fouling resistance R_f is plotted over the experimental time (Kazi, 2001).

The data obtained in this work show good agreement with the data of Kazi et al. concerning induction time and heat transfer augmentation. After 90 hours the experiment was terminated unintentionally, as the controller of the pump drive turned off automatically. This partial experiment was not repeated as the correspondence with the data of Kazi et al. for that portion of the curve was good.

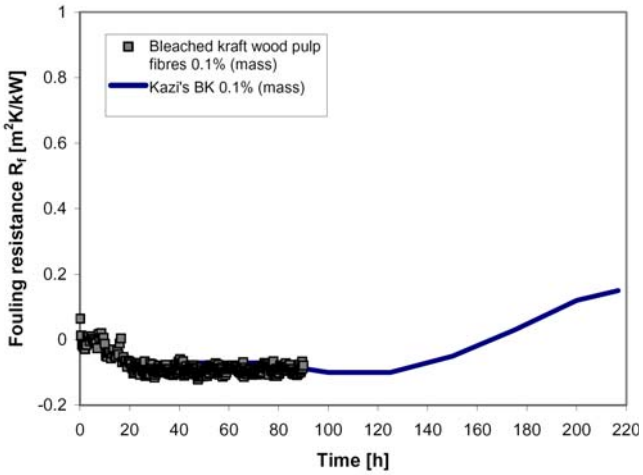

Fig. 4: Fouling resistance data and the Kazi et al. (2001) curve as a function of time for bleached kraft pine pulp fibres at a mass concentration of 0.1%. $CaSO_4$-concentration 3.6g/l, T_b=40^{0}C, ΔT=15K (Kazi, et al., 2001)), 20K (this work), v=0.4m/s.

Man-Made Synthetic Fibres – Rayon and Acrylic

Rayon

The fouling curves obtained with both the rayon fibres – Rayon I and Rayon II – are shown in *Fig. 5* as a plot of fouling resistance R_f against experimental time. For the purpose of comparison, the fouling curve of the fibre-free solution obtained by McShane with the same test rig and with identical parameters is included here. Clearly there is no induction period t_D, no heat transfer augmentation t_A and no asymptotic behavior. Hence the fouling resistance exceeds the values of the ultimate fouling resistance for the fibre suspensions.

All suspension curves show the typical shapes obtained with fibre suspensions in a fouling solution as obtained by previous workers (e.g. Kazi, et al., 2001). After the induction period t_D where no fouling is obtained the fouling resistance becomes negative which is the so-called *period of heat transfer augmentation* t_A. After this period the fouling resistance becomes positive again and finally reaches an asymptotic fouling resistance level $R_{f,\infty}$.

With both Rayon fibres, experiments were conducted at a fibre volume concentration of 0.075%. A further experiment was performed with Rayon I fibres at 0.125%. After a modification of the test section both experiments at a volume concentration of 0.075% were repeated (indicated with * in the inset box in *Fig. 5*). The modification was carried out to improve heat conduction between the band heaters and the outer test pipe surface by replacing the interleaved aluminum foil with a thermal conducting compound. The modification resulted in lower initial heat transfer coefficients α_0 as a less power output to the band heaters was needed to maintain the constant

temperature difference between the surface and the bulk temperature. Furthermore, the induction period t_D in both experiments was prolonged, which may be due to the more evenly distributed heat over the pipe surface and hence the reduction in 'hot spots'. The curves also reached a lower resistance level $R_{f,\infty}$ compared with the original setup, which may be related to the poorly adherent fouling layer obtained as a consequence of the planned modification.

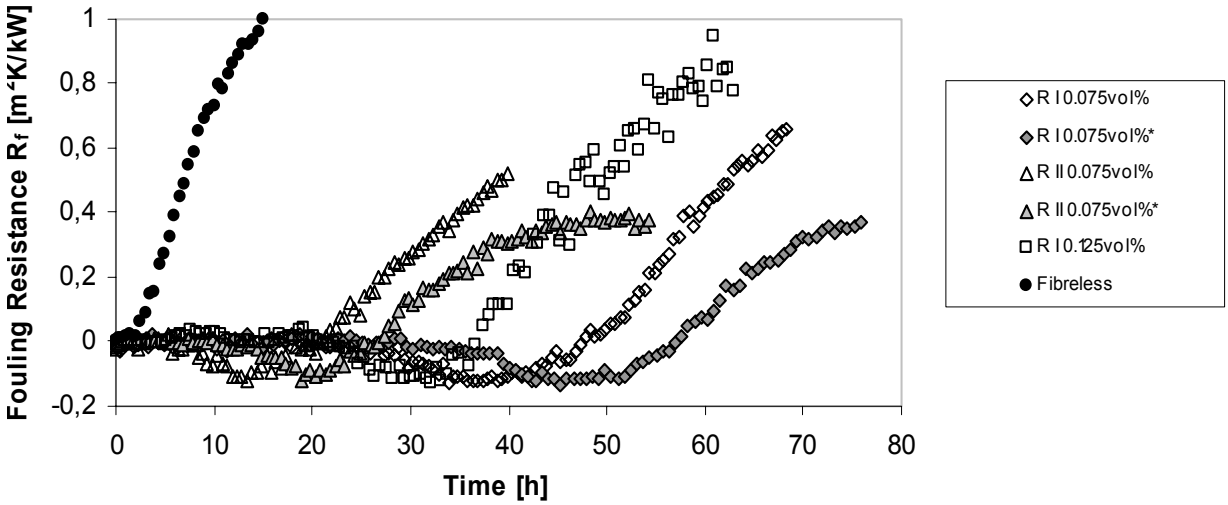

Fig. 5: Fouling resistance curves as a function of time for rayon fibres at different concentrations ($C_{f,vol}$=0.075-0.125%) and diameters (D=25µm, 32.5µm). $CaSO_4$-concentration 3.6g/l, T_b=40°C, ΔT=20K, v=0.4m/s.

Acrylic

The results of the experiments with the acrylic fibres are depicted in *Fig. 6* in the usual way. The acrylic fibre experiments were performed at a fibre volume concentration of 0.075% in both the original and the modified test sections. Further experiments were conducted with fibres at a volume concentration of 0.086% (equivalent to 0.10% fibre mass concentration) and also with traces of fibres.

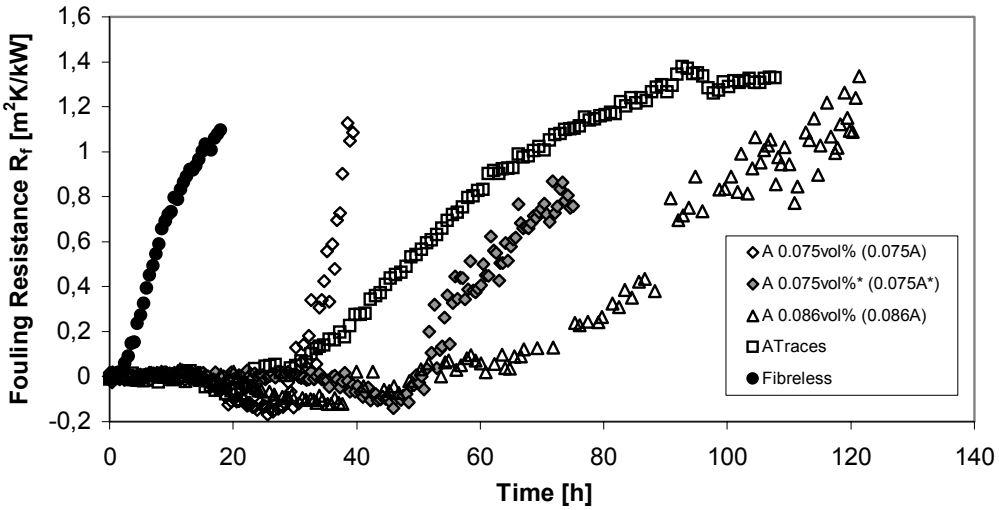

Fig. 6: Fouling resistance curves as a function of time for acrylic fibres of D=20µm at different concentrations ($C_{f,vol}$=0.075%/0.086%). $CaSO_4$-concentration 3.6g/l, T_b=40°C, ΔT=20K, v=0.4m/s.

Analysis of the Fouling Layer

A considerable amount of fibre was found to be embedded into the fouling layer. The appearance of the layer when looking lengthwise into the pipe is shown diagrammatically in *Fig. 7*. Fibres on the top of the fouling layer protrude radially out of the fouling deposit surface into the bulk of the flowing fluid.

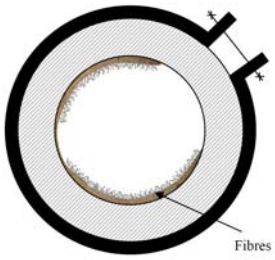

Fig. 7: Appearance of the fouling layer, when looking in longitudinal direction of the pipe.

On completion of the acrylic fibre experiment at 0.075 vol %, the flow loop was emptied and the fouling layer dried using the band heaters. The deposit was physically removed from the pipe surface and examined under the microscope as shown in *Fig. 8*. A typical view of the fouling deposit adjacent to the pipe wall is shown in the left side of the figure showing there are no fibres protruding from the deposit surface. A view of the fouling surface on the fluid-side with fibres protruding is shown in the right of the figure. The thickness of the fouling layer was approximately 0.5 – 1.5mm.

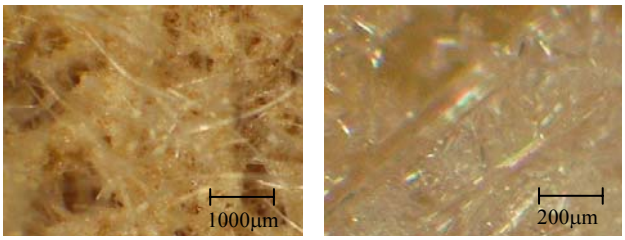

Fig. 8: Appearance of the fouling layer, from the pipe surface side and the fluid side..

Overview of the obtained fouling parameters

Table 3 shows all fouling parameters of the experiments plotted in *Fig. 4* to *6*.

Table 3: Fouling parameters obtained for two rayon fibre types and one acrylic fibre type at different fibre volume concentrations.

	t_D [h]	t_R [h]	$R_{f,min}$ [m²K/kW]	ΔS_0 10^{-3} [m²K/kWh]	$R_{f,\infty}$ [m²K/kW]	α_0 [W/m²K]
Rayon I 0.075vol%	24	47	0.120	33.6	ca. 0.8	1790
Rayon I 0.075vol%*	35	59	0.113	28.7	0.4	1499
Rayon I 0.125vol%	21	38	0.128	41.4	ca. 0.8	1840
Rayon II 0.075vol%	6	20	0.111	31.0	ca. 0.8	1800
Rayon II 0.075vol%*	14	27	0.109	30.1	0.4	1514
Acrylic 0.075vol%	15	30	0.143	77.2	ca.1.4	1848
Acrylic 0.075vol%*	38	51	0.114	55.9	0.9	1551
Acrylic 0.086vol%	18	48	0.093	11.9	ca. 1.4	1892
Acrylic Traces	15	25	0.071	19.5	1.4	1793
Wood pulp Pine 0.1mass%	10	>90	0.100	-	-	2081

* modified test section

DISCUSSION

Relationships among initial heat transfer coefficient, fibre stiffness, and fibre concentration

The initial values of heat transfer coefficient allow conclusions to be drawn on how the fluid flow (especially the sub-laminar layer near the wall) is modified by the fibres, especially by fibre stiffness and fibre concentration, before any fouling reaction can occur (Duffy and Lee, 1978; Duffy, 2003).

The initial heat transfer coefficient α_0 for each experiment was found from the arithmetic average of the values during the induction period t_D. As shown in *Fig. 9* all initial heat transfer coefficients α_0 obtained with fibres added to the solution were higher than for the fibre-free solutions (α_0 of 1,750 W/m2K) regardless of fibre concentration and type. The highest value was obtained for the wood pulp fibres at a mass concentration of 0.1% with 2081 W/m²K, followed by the acrylic fibres at 0.086vol% with 1892 W/m²K. Further it can be seen that regardless of the amount of fibre added heat transfer is augmented when compared with the fibre-free solution.

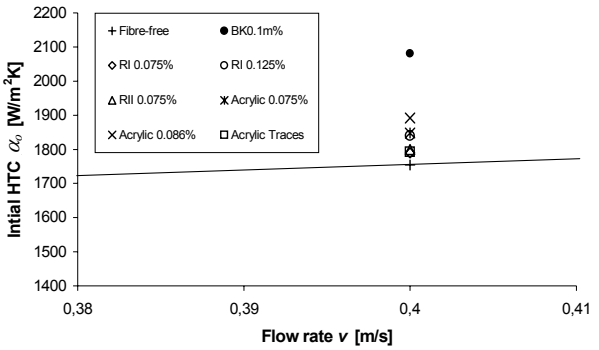

Fig. 9: Initial HTC values as a function of flow rate, fibre type, and fibre concentration.

The level of heat transfer coefficient values for the man-made fibres increased both with increasing fibre volumetric concentration and fibre stiffness, as shown in *Fig. 10*. The heat transfer coefficients obtained with the new arrangement of the band heaters were multiplied by a determined factor of 1.2 to adjust them to the values obtained with the original heater arrangement.

Heat transfer was highest with the stiffest acrylic fibres, followed by the thicker Rayon II, and finally Rayon I with the lowest transfer of heat. This trend can clearly be seen at a fibre concentration of 0.075vol%, where values for all three fibre types validate this trend.

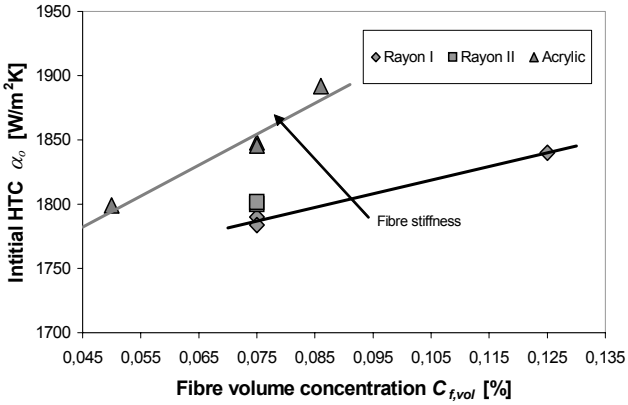

Fig. 10: Initial HTC values as a function of volumetric concentration and fibre type.

Clearly the values of heat transfer coefficient increase with both fibre stiffness and fibre concentration when compared with water alone. It can be concluded that for the range of fibre concentrations and the flow rates used in here, the mechanism of momentum transmission near the wall between neighbouring fibres and turbulent eddies dominates over the mechanism of turbulence fibre damping. Fibres act as micro-mixers affecting energy dissipation and mass transfer minimisation (Duffy, 2003). This predominant turbulence enhancing mechanism not only increases the heat transfer but also the mass transfer to the surface and the laminar sub-layer thinning increases the concentration and temperature gradients adjacent to the wall.

As the deposition of $CaSO_4$ is considered to be both reaction and mass-transfer controlled, it is difficult to assess the level and extent that each mechanism influences the deposition rate. However it is apparent that the wood pulp fibres with the highest initial heat transfer coefficients had – apart from Rayon II at 0.075% – the shortest induction period t_D; yet at the same time the longest roughness delay period t_R. This is a strong indication that the modification of the laminar sub-layer is a dominant feature especially during the induction period. Once a fouling layer has developed this no longer dominates the heat transfer mechanism as the longer roughness delay period t_R with wood pulp fibres show.

Relationship between ultimate fouling resistance and fibre stiffness

The values of ultimate fouling resistances $R_{f,\infty}$ for the experiments at a fibre volume concentration of 0.075% were plotted against the parameters which describe fibre flexibility and fibre stiffness (namely the fibre deflection w' and the calculated fibre stiffness S_{calc}) as depicted in *Fig. 11* and *Fig.* 12, respectively. Though the experiment with Rayon II fibres (test section in the original state) were stopped by a power cut before the ultimate fouling resistance became constant, it could be determined sufficiently accurately. A data point (indicated grey) on the level of the Rayon I fibre was estimated.

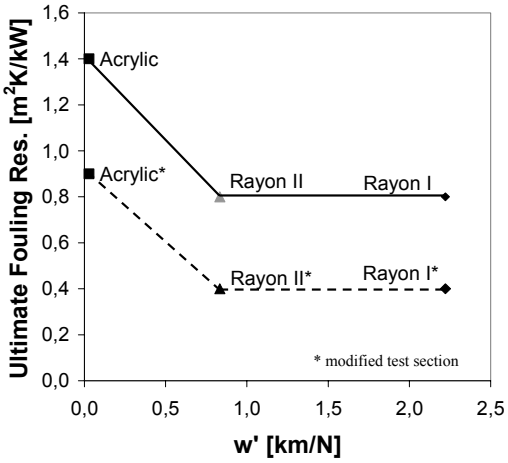

Fig. 11: Correlations between the fibre deflection w' and $R_{f,\infty}$ at $C_{f,vol}$ = 0.075%.

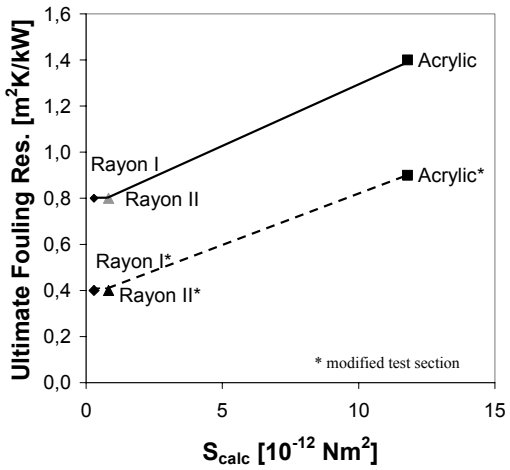

Fig. 12: Correlations between the calculated fibre stiffness S_{calc} and $R_{f,\infty}$ at $C_{f,vol}$ = 0.075%.

Correlations between the ultimate fouling resistance $R_{f,\infty}$ and the fibre deflection w' and the calculated fibre stiffness S_{calc} can be seen in these figures. Higher deflections w' result in a decrease in the ultimate fouling resistance $R_{f,\infty}$, whereas $R_{f,\infty}$, increases with increasing calculated stiffnesses S_{calc}. The correlation with the latter parameter S_{calc} is the most obvious one, as in the w'-diagram a distinct plateau between the data points of both rayon fibre types is apparent. Out of these diagrams it can be concluded that the more flexible fibres produce a lower ultimate fouling resistance and are therefore more effective in mitigating fouling.

Additionally it seems that the inherent fibre stiffness is more significant than the geometrical properties in effecting a lower ultimate fouling resistance $R_{f,\infty}$. The following mechanism is proposed to explain this. As fibres were found to be embedded into the fouling layer and have a very low thermal conductivity (e.g. 0.19-0.24W/mK for acrylic) themselves, they contribute together with the calcium sulphate to the fouling resistance. It can be assumed that the resistance of the removal of the fouling layer by hydrodynamic shear forces increases with fibre stiffness as the network strength of the embedded fibres increases with fibre stiffness (Switzer and Klingenberg, 2004). Hence, a fouling layer with stiffer fibres can build up to a higher thickness, before the deposition and the removal rate become equal, i.e. the fouling resistance becomes constant with time. Also, as the fibres were found to protrude into the bulk, they act as a mat in which other fibres can get caught. Therefore, fibres with a higher stiffness are likely to be much more effective as they can resist better the shear forces, which press the fibres down flat to the surface. Since the mechanism of abrading the fouling layer by fibres exists in this fouling stage, (stiffer fibres are believed to be more effective in achieving this (MacShane, 2004)), then it is clear that this mechanism is not the dominant mechanism.

Relationship between ultimate fouling resistance and fibre volume concentration

The ultimate fouling resistance $R_{f,\infty}$ was found to be independent of fibre volume concentration $C_{f,vol}$ as shown in *Fig. 13.*

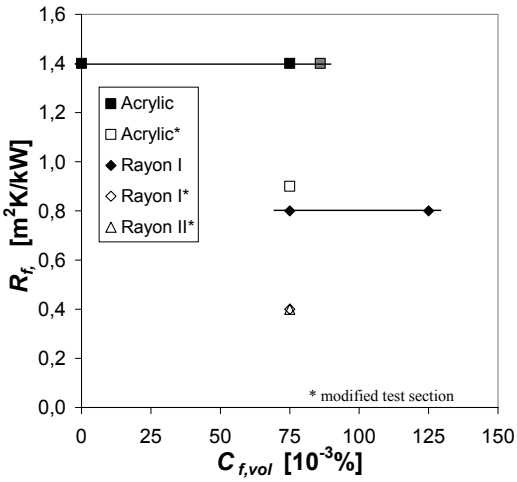

Fig. 13: Correlation between the fibre volume concentration $C_{f,vol}$ and the ultimate fouling resistance $R_{f,\infty}$.

In all three experiments conducted with acrylic fibres at different volume concentrations (from traces of fibres to 0.086vol%), the ultimate fouling resistance $R_{f,\infty}$ reached the same asymptotic level at about 1.4 m^2K/kW with the original setup of the test section. There were also no differences in the ultimate fouling resistance $R_{f,\infty}$ with Rayon I at 0.075vol% and 0.125vol% and in both cases a value of approximately 0.8 m^2K/kW was obtained. This observation is not in agreement with observations of the former workers, who found varying ultimate fouling resistances at different fibre concentrations.

Relationship between ultimate fouling resistance and initial heat transfer

MacShane (2004) observed a trend that a higher initial heat transfer coefficient results in a higher ultimate fouling resistance. This trend was also observed here and was apparent between the rayon fibre types and the acrylic fibres. The acrylic fibres produced both higher initial heat transfer coefficients and ultimate fouling resistance levels compared to the rayon fibres at the same fibre volume concentration of 0.075% as depicted in *Fig 14*. The fact that the initial heat transfer coefficients of Rayon I and Rayon II were very close and both

obtained equal ultimate fouling resistances is a further confirmation of this trend.

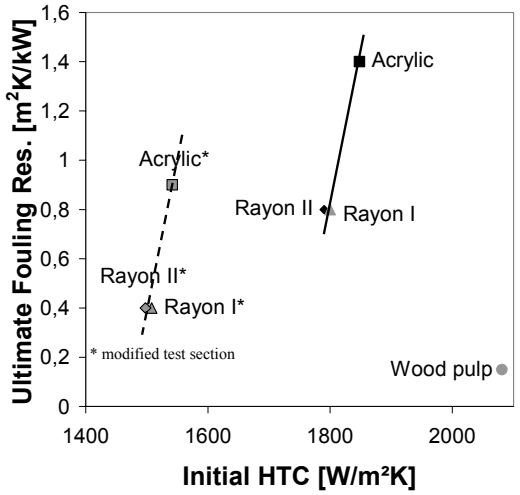

Fig. 14: Correlation between the Initial heat transfer coefficient α_0 and the ultimate fouling resistance $R_{f,\infty}$.

This trend was not observed with the same fibre type as an increase in volume concentration led to an increase in the initial heat transfer α_0, but the ultimate fouling resistance $R_{f,\infty}$ remained constant. Wood pulp fibres are different. As shown in *Fig. 9,* the initial heat transfer coefficient α_0 for bleached Kraft pine fibres at a mass concentration of 0.1% (larger concentration than used for the man-made fibres at 0.075vol%) is considerably higher, whereas its ultimate fouling resistance (Kazi et al. value of 0.15W/m²K is assumed (see *Fig. 4*)) – is significantly lower.

The trend between the initial heat transfer and the ultimate fouling resistance may be linked to fibre stiffness. Stiffer fibres were found both to increase the initial heat transfer (see *Fig. 10*) and produce higher ultimate fouling resistance levels (see *Fig. 12*). Regarding these results, MacShane's conclusion to find the most effective fibre to mitigate fouling (assuming the ultimate fouling resistance is considered the decisive parameter of fouling mitigation) by conducting heat transfer experiments instead of time-consuming fouling experiments with different fibres could be substantiated and additionally refined.

Overview of possible fibre related mechanisms

Several mechanisms during fouling with fibres are thought to prevail. The known ones are listed below. Not every mechanism has to be in existence simultaneously in every fouling period.

- Fibres abrade the forming nuclei or the initial fouling layer,
- Fibres act as nucleation sites and take away the some fouling matter,
- Fibres enhance the roughness of the forming fouling layer due to the abrading mechanism,
- Fibres modify the laminar sub-layer as fibres interconnect with turbulent eddies and increase/decrease turbulence. This influences mass transfer and temperature and concentration gradients,
- Fibres are embedded in the forming fouling layer and affect further fouling developments.

CONCLUSIONS

The more flexible rayon fibres in suspension produced lower ultimate-fouling resistance values than the stiffer acrylic fibres in agreement with previous workers. It was found that fibres become embedded in the fouling layer and hence contribute to the fouling resistance themselves. The free ends of the embedded fibres protrude into the bulk flow and trap fibres flowing in the bulk more easily. The more flexible fibres are flattened by the current forces and thus are less able to trap the flowing fibres. This uniquely 'structured' layer can resist hydrodynamic shear forces which thin the fouling layer.

NOMENCLATURE

$C_{f,vol}$	volumetric fibre concentration, m³/m³
D	fibre diameter, m
E	E-Modul, N/mm²
I_0	area moment of inertia, m⁴
L′	fibre length, m
$\dot{q}$	heat flux density, W/m²
R_f	fouling resistance, m²K/W
$R_{f,\infty}$	ultimate/asymptotic fouling resistance, m²K/W
S_{calc}	calculated fibre stiffness, Nm²
T_b	bulk temperature, °C
T_w	wall temperature, °C
t_D	induction period, h
t_R	roughness delay period, h

Greek symbols

α	heat transfer coefficient, W/m²K
α_0	initial heat transfer coefficient, W/m²K

Subscript

f	fibre or fouled
calc	calculated
susp	suspension

REFERENCES

Duffy, G. G. and Lee, P. F. W., 1978, Drag reduction in the turbulent flow of wood pulp suspensions. *Appita Journal*, vol. 31, no. 4, pp. 280-286.

Bansal, B. and Müller-Steinhagen, H., 1993, Crystallization fouling in plate heat exchangers. *Transactions of the ASME, Journal of Heat Transfer*, vol. 115, no. 3, pp. 584-91.

Middis, J., Paul, S. T., Müller-Steinhagen, H. M., and Duffy, G. G., 1998, Reduction of heat transfer fouling by the addition of wood pulp fibers. *Heat Transfer Engineering*, vol. 19, no. 2, pp. 36-43.

Kazi, S. 2001, *Heat Transfer to Fibre Suspensions - Studies in Fibre Characterisation and Fouling Mitigation*. Ph.D., Department of Chemical and Material Engineering, The University of Auckland, Auckland.

Kazi, S., Duffy, G. G., and Chen, X. D., 2001, Heat transfer fouling mitigation with wood pulp fibres, in *Heat transfer fouling Conference*, no. 5, Davos, Switzerland, 2001.

Kazi, S. N., Duffy, G. G., and Chen, X. D., 2002, Fiber-modified scaling in heat transfer fouling mitigation. *Chemical Engineering Communications*, vol. 189, no. 6, pp. 742-758.

Duffy, G. G., 2003, The significance of mechanistic-based models in fibre suspension flow. *Nordic Pulp and Paper Research Journal*, vol. 18, no. 1, pp. 74-80.

MacShane, K. S. 2004, *Heat Transfer to Model Fibre Suspensions - Fibre Quality Prediction and Fouling Mitigation*. M.Eng., Department of Chemical and Material Engineering, The University of Auckland, Auckland.

Switzer, L. H. and Klingenberg, D. J., 2004, Flocculation in simulations of sheared fiber suspensions. *International Journal of Multiphase Flow*, vol. 30, no. 1, pp. 67-87.